Embroidered Resistive Pressure Sensors: a Novel Approach for Textile Interfaces

Roland Aigner*, Andreas Pointner*, Thomas Preindl*, Patrick Parzer, Michael Haller
mi-lab@fh-hagenberg.at
Media Interaction Lab, University of Applied Sciences Upper Austria

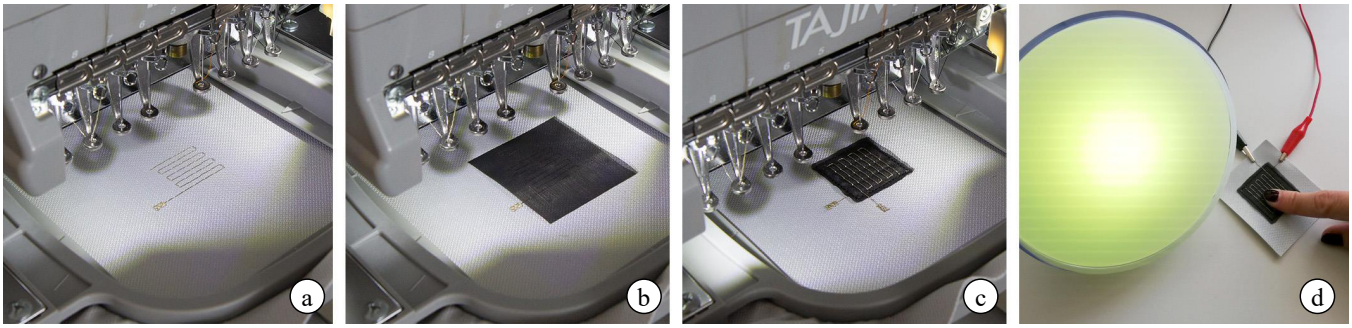

Figure 1: The workflow of implementing an embroidered pressure sensor: stitching an electrode to a base material using a conductive yarn (a), adding a resistive fabric (b), and stitching another electrode with conductive yarn (c). The resulting sensor's resistance readings may be used for arbitrary controls (d).

ABSTRACT

We present a novel method for augmenting arbitrary fabrics with textile-based pressure sensors using an off-the-shelf embroidery machine. We apply resistive textiles and conductive yarns on top of a base fabric, to yield a flexible and versatile continuous sensing device, which is based on the widespread principle of force sensitive resistors. The patches can easily be attached to measurement and/or computing devices, e.g. for controlling accessories. In this paper, we investigate the impacts of related design and fabrication parameters, introduce five different pattern designs, and discuss their pros and cons. We present crucial insights and recommendations for design and manufacturing of embroidered pressure sensors. Our sensors show a very low activation threshold, as well as good dynamic range, signal-to-noise ratio, and part-to-part repeatability.

CCS CONCEPTS

• **Human-centered computing** → **Interaction devices**; **Haptic devices**.

KEYWORDS

Embroidered Force Sensitive Resistance; Embroidery; Space-Filling Patterns; Textile Sensor; Smart Textiles

CHI '20, April25–30, 2020, Honolulu, HI, USA

ACM ISBN 978-1-4503-6708-0/20/04…$15.00
https://doi.org/10.1145/XXXXXXX.XXXXXXX

ACM Reference Format:
Roland Aigner*, Andreas Pointner*, Thomas Preindl*, Patrick Parzer, Michael Haller. 2020. Embroidered Resistive Pressure Sensors: a Novel Approach for Textile Interfaces. In *CHI Conference on Human Factors in Computing Systems (CHI '20), April 25–30,2020, Honolulu, HI, USA.* ACM, New York, NY, USA, 11 pages. https://doi.org/10.1145/XXXXXXX.XXXXXXX

1 INTRODUCTION

The handcraft of textile production is sometimes attributed as one of the first technologies of human history. Consequently, textiles are omnipresent in humans' environment for millennia, throughout all parts and cultures of the world, most visibly in the form of clothing. By now, we are literally surrounded by textiles, since they are also found on furniture, walls, and floors, in vehicles, but also in very much concealed forms, such as fiber-reinforced composites. This quality of ubiquity and versatility poses an ideal vantage point for pushing Mark Weiser's frequently quoted vision of Ubiquitous Computing [34]. In this spirit, professionals and hobbyists have recently moved on from e-textiles (incorporating elements for heating, lighting, etc.), and started incorporating interactive functionalities into textiles by weaving, knitting, and embroidering. Apart from availability, numerous aspects of textiles pose great advantages for function and comfort, such as flexibility, elasticity, breathability, and pleasant haptic qualities.

In this paper, we focus on the process of embroidery, which is the craft of applying yarn to a base fabric, originally used for aesthetic purposes. The development of machine-embroidery made it a fundamental tool of modern textile finishing for mass production,

*Authors contributed equally to this research.

still providing advantages like customization and repeatability. Arguably, this caused its spread to technical applications in the fields of engineering [31], medicine [2], and smart textiles [19]. Beyond advantages in industrial production, we deem the technique ideal for rapid prototyping of textile sensors and circuitry.

We present a method for implementing pressure sensor patches on top of existing weaves or knits. In contrast to solutions with discrete pressure sensitive *points* [22], we aim for sensor *areas*, enabling to create arbitrary shapes and sizes. We utilize a commercial embroidery machine (cf. Figure 1), which allows to specify a variety of parameters to control the behavior of the resulting sensor. We therefore examine these parameters with respect to their impact on the sensor's responsiveness and dynamic range. Moreover, we investigate a number of patterns, which are highly scalable in size, and report on their advantages and disadvantages. We highlight best practises to embroider resistive textile sensors and complete with a description of two applications demonstrating potential use cases.

In summary, the main contributions of this paper are:

- A description of a method for rapid prototyping of pressure sensors via a commercially available embroidery machine.
- Findings of an experiment, investigating design and manufacturing parameters, which are affecting the sensors' performance.
- Study and analysis of five space-filling patterns for generating scalable pressure sensor patches.
- Implications and best practices for design and manufacturing, in particular regarding handling of conductive yarn in context of embroidery.
- Example applications demonstrating the embroidered pressure sensors and the feasibility of our approach.

2 RELATED WORK

Textile sensing is an extensive area of research addressing the acquisition of analog or digital information from textiles by means of electronic measurement. A subdomain is dealing with the detection of changes in pressure, predominately using capacitive and resistive approaches. Both sensing methods are viable for pressure and touch sensing with their respective benefits and drawbacks originating from their fundamentally different working principles. The suitable sensing method therefore often depends on the actual use cases. In our work, we focus on resistive pressure sensors utilizing the advantages that come with that approach.

2.1 Textile Pressure Sensors

Resistive textile sensors are usually composed of two conductive electrodes separated by a resistive sheet [27, 32, 36]. Often, they augment everyday objects with sensing capabilities. Rofouei et al. [27] constructed an array of pressure sensors using a resistive fleece, placed between two conductive layers. The sensor grid could infer shape, position and weight of an object placed on it. Using the same resistive textile *eCushion* [36] built a smart cushion for sitting posture analysis. Similarly, Shu et al. [16] implemented a resistive textile pressure sensor array for in-shoe sensing, electrically connected by conductive yarn, which is adhered to the readout electronics. Researchers have developed a multitude of resistive textile sensor arrays based on a multi-layer approach [6, 7, 23, 29, 32, 38]. *SmartMat* [32] is integrating textile pressure sensors into exercise mats to recognize and count several types of exercises. *GestureSleeve* [29] presents a touch-enabled textile placed on the forearm, enabling interaction via gestures, such as swipes or taps. *FlexTiles* [23] uses a stretchable three-layer sensor, to detect pressure on prosthetic limbs [15], or detecting a wide range of gestures on textiles [24]. There are notable exceptions to these multi-textile-layer approaches. *RESi* [22] combines conductive and resistive properties on a yarn level. Saenz-Cogollo et al. [28] built a resistive sensor mat by embroidering conductive yarn onto a non-conductive textile and stamping a conductive polymer onto the yarn junctions to enable pressure sensing.

Our sensor design builds upon mentioned research and offers comprehensive design details for applications where multi-scale sensors and a comprehensible manufacturing process from fabric to function are required.

2.2 Machine Embroidery

Embroidery has been one of the first fabrication techniques used in the field of smart textiles. In their pioneering work, Post et al. [26] used it to create conductive electrodes for capacitive sensing, inspiring other works and thereby casting the seed for the prospective field of smart textiles. Embroidery was utilized for generating multi-layered capacitive sensing structures [20], connections between textile wiring and rigid electronic substrates [17], integrating electromyography electrodes into clothes [30], creating antennas [1, 5, 13, 33] and fabricating textile coils for magnetic resonance sensors [21]. Also interaction-centered applications, such as pinch gesture recognition on textiles [11, 14], have been investigated. Researchers also combined aesthetics with function in embroidered pattern resistors [10] and realized imaginary computing technologies by embroidering logic gates with ornamental patterns [25].

Addressing the wide range of application specific papers, we seek to offer a fabrication centered approach, to facilitate the design and manufacturing process of textile pressure sensors for future researchers, practitioners, and makers.

2.3 Customized fabrication

From early on, the field of smart textiles showed a strong overlap of academic research, art practices, education, and the DIY community. The extensive collection of projects from Satomi and Perner-Wilson, combining textile crafts with electronics on their platform *Kobakant*[1], demonstrated the virtue of hands-on fabrication in the domain of personal fabrication. Acknowledging the demand for personal fabrication methods in the field of smart textiles, a growing group of researchers addresses this topic in the context of weaving [9] and embroidery [12].

Aligning with their goals, we try to narrow the gap between textile fabrication and electronic engineering to foster collaboration and enhance mutual understanding in both fields.

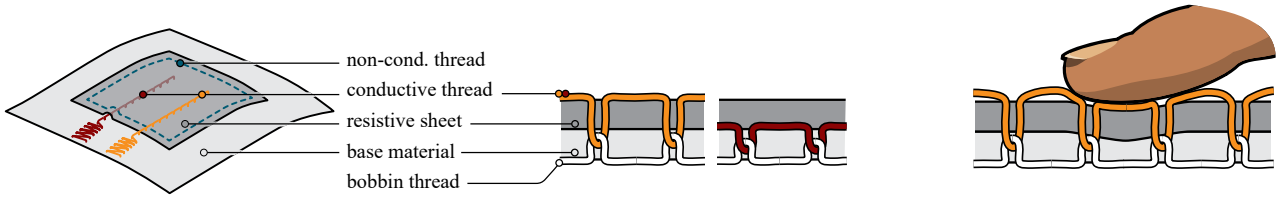

Figure 2: The basic components of our embroidered pressure sensor (left), showing bobbin thread holding the conductive yarn. The degree of contact and compression of yarn and resistive material is the most contributing factor to the change of resistance (right): when pressure is applied, the contact area between yarn and resistive material rises (right).

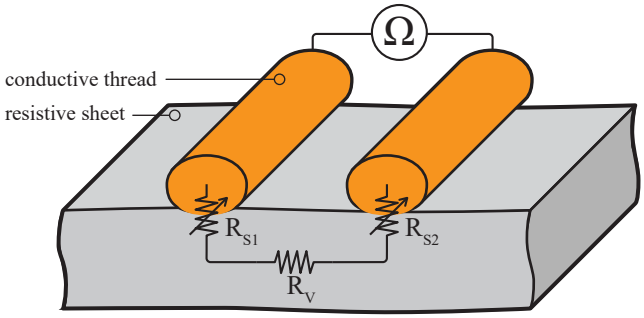

Figure 3: The overall resistance is the sum of volume resistance and two surface resistances, resulting in $R_{total} = R_V + R_{S1} + R_{S2}$.

3 FORCE SENSITIVE RESISTANCE

Our textile sensor is based on the principle of *Force Sensitive Resistors* (FSR), which are used in different applications for several decades [8]. An FSR represents a continuous electrical controller, whose electric resistance decreases gradually as pressure is applied. In our implementation, two electrodes are put in contact with a resistive material (cf. Figure 3).

From an electrical point of view, the sensor's overall resistance is the sum of the material's volume resistance R_V and the surface resistances R_{S1} and R_{S2} resulting from the contact areas of each of the electrodes. While volume resistance is mostly constant for a given sensor, the surface resistance is varying when pressure is applied, as a result of the interface effect [35].

3.1 Embroidered Force Sensitive Resistor

The most common stitch in machine embroidery is the *lockstitch*, which interlocks an upper and a lower (*bobbin*) thread using a rotary hook.

For the embroidered sensors, we augment a *base fabric* substrate with pressure sensing capability, employing a *conductive yarn* as upper and a *non-conductive yarn* as bobbin thread (cf. Figure 2). In one of three possible approaches, the base fabric is covered by the *resistive material*, which is then fixated along the edges using a regular, non-conductive yarn, in order to prevent it from shifting out of place. Subsequently, the electrodes are stitched on top. Contrary, electrodes can also be stitched below the resistive material or in alternating order, as we will demonstrate later.

3.1.1 Base fabric. A crucial property for manufacturing is the thread count of the base fabric, as it affects the precision of the embroidered pattern: denser materials enable for more accurate positioning of stitches. While not affecting the sensor's electrical properties, thread count affects the minimum electrode distance that can be achieved. Moreover, a so-called *backing* or *stabilizer* (usually a non-woven fabric) is commonly applied to the backside of the base material, to prevent warping caused by the pull of the embroidery yarns, which in our case would result in stressing the sensor, introducing noise indistinguishable from actual applied pressure. Also, stretching the base fabric can cause the electrodes to tear, rendering the sensor permanently defective. For our sensors, we decided for the BadgeTex 2900 twill with 330 g/m^2, as it allows for sub-millimeter precision in positioning stitches and shows little tendency to frail when trimmed. It comes already with the top cloth pressed onto a polyester fleece stabilizer, to prevent warping.

3.1.2 Resistive fabric. Regarding the resistive fabric, we investigated several materials suitable for embroidery. Options include knitted and woven fabrics, fleeces, and foams. We closely inspected the Eeonyx EeonTex LTT-SLPA 20 k knit and the SEFAR CARBOTEX 03-82 CF weave (cf. supplementary material). During our tests, we noticed that the elastic Eeonyx shows anisotropic performance, due to the inherent surface structure of a knit. Additionally, the behavior largely varies, depending on which side is facing up. Therefore, we decided to use the CARBOTEX, since it did not show direction dependent behavior. Note that there are also weave variants not fully made of carbonized threads, which potentially renders them direction dependent and inhomogeneous.

3.1.3 Stitching of electrodes. We informally evaluated 39 commercially available conductive yarns, inspecting electrical resistance, mechanical abrasion, and suitability for machine embroidery. Detailed information and results of this evaluation can be found in the supplementary material. We found the Madeira HC40 as the ideal yarn for our requirements, since it is specially designed for embroidery machines and proved durable during our tests. Moreover, it showed relatively low electrical resistance of 127 Ω/m. As a bobbin thread, we used an Amann ISABOB 100% Polyester pre-wound bobbin thread.

As the resistive fabric is of uniform thickness, and assuming parallel electrodes of equal length, the resulting resistor can be

[1] www.kobakant.at/DIY/

modeled as a cuboid with specific electrical resistance ρ. In this case, the longitudinal resistance between the two electrodes is

$$R = \rho \frac{d}{tl}, \tag{1}$$

where t is the resistive material's thickness, l is the length of the respective electrode's trace length on-top of the resistive material, and d is the distance between the two electrodes (cf. Figure 4).

4 SENSOR EVALUATION

In the following, we describe an evaluation of our pressure sensor design with respect to design and fabrication parameters. In particular, we were interested in how these parameters affect resistance once we apply pressure (cf. Figure 4a). Therefore, we tested variations of a primitive sensor by placing weights on top. For these patches, we modified several parameters we considered relevant for their performance: due to the general definition of electrical resistance (cf. Equation 1) and since material thickness t is constant, the most relevant properties in our scenario are *electrode distance d* (1 mm, 2 mm, 4 mm, …, 32 mm) and *electrode length l* (10 mm, …, 60 mm) (cf. Figure 4a,b). Furthermore, we investigate *stitch length s* (1 mm, 2 mm, 5 mm), which is the distance between two stitches, mostly affecting the compression of yarn and fabric at rest[2] (cf. Figure 4c). We also tested different modes of *electrode layering*, meaning if both electrodes are stitched (i) *on top*, or (ii) *below* the CARBOTEX sheet, or (iii) in *mixed*, i.e. alternating order (cf. Figure 4d). As discussed later, some of our pattern layouts feature electrode intersections and double stitches, therefore we also tested those: *intersections* (none vs. one) require *mixed* electrode layering and are established by guiding the upper electrode across the lower one (cf. Figure 4e). *Double stitches* (single vs. double) refer to parts of the electrode trace that are stitched twice, e.g. by performing a U-turn and following the exact same trace backwards (cf. Figure 4f).

4.1 Apparatus

For our experiments, we manufactured patches consisting of two parallel straight electrodes of equal length and fixed the CARBOTEX resistive fabric with a non-functional thread (65×65 mm^2). We fabricated 6 samples for each variation to cancel out fabrication imprecisions in our data, resulting in an overall of 108 patches. Note that for testing electrode lengths, we varied the size of the resistive sheet instead of the electrode and fixed it only at the outer sides, left and right (cf. Figure 4b). We did this to precisely control the effective trace length, i.e. the extent of the stitch intersecting with the CARBOTEX, so imprecisely trimmed seam would not affect the results.

For evaluation, we mounted each of the samples flat on a rubber sheet for good support, and placed a PMMA-plate (60×60 mm^2, so it would not rest on the fixation stitch) on top, for equally distributing pressure all over the sensor area (cf. Figure 4a). All sample patches were generated with a Tajima SAI[3], in combination with the Creator software from Pulse Microsystems Ltd.

[2]Machine controlled thread tension is also contributing to compression, however it has to be properly balanced to yield a sound stitch and therefore allows little scope for variation.
[3]MDP-S0801C

4.2 Procedure

For measuring resistance values, we used a Tektronix Keithley 2401 SourceMeter Instrument, attached with crocodile clips for reliable and consistent connection. We first measured each sample without pressure applied, then we put on the PMMA-plate (12 g) and successively added weights of 100 g, 200 g, 500 g, 1000 g, and 2000 g on top of the plate. In order to compensate for drift, we waited for 5 s before removing and placing the next weight. For data analysis, we chose a measurement value after 3 s of inaction, so the resistance value was reasonably settled with RSD[4] < 0.5 % in ±0.5 s.

4.3 Results

In particular, we investigated the resistance difference between zero-load and maximum weight, henceforth used as a measure for *dynamic range*. We judged high ranges as superior since our intention was to implement a textile sensor similar to widespread FSRs (e.g. FSR 402), which exhibit similar characteristics, and are therefore easily applied in combination with straightforward measurement electronics (e.g. via voltage dividers). Another aspect we consider is the resistance when the sensor is not stressed, which we call the *resting resistance*. While not necessarily a measure of sensor performance, it may affect the choice of readout electronics. Beyond absolute values, the *relative dynamic range* provides information about the sensitivity at low and high pressure levels. We calculate relative values by normalizing measurements by the respective resting resistance.

Our results are presented in Figure 5. Overall, highest resistance values were observed for patches with electrode layering methods *mixed* and *below*, with a high RSD of up to 69 % at rest. Otherwise, RSD within patch configuration was mostly below 20 %, with an exception of patches for testing electrode length, which showed noticeably high RSD of 18 % to 31 %. Samples with d = 1 mm were also highly erratic (RSD = 15 %), which we speculate is a result of their tendency to short, especially when stressed, as their electrodes are too close. Due to those inconsistencies, we decided to remove outliers for further data analysis, so we deleted two measurements per configuration at maximum, which resulted in 12 % of our total patches.

4.3.1 Electrode Distance. We observed a strikingly linear relation between resistance and electrode distance, confirming factor d in Equation 1. Dynamic range increased slightly with higher electrode distances, providing beneficial conditions for sensing.

Based on the presented results, we recommend to use this parameter to control the resting resistance. Furthermore, we infer that high electrode distances are preferable, as they provide higher dynamic range. The maximum distance is however depending on the use case, since it should not exceed the minimum actuator size.

4.3.2 Electrode length. The data confirms the inverse relation of resistance and electrode length l in Equation 1. Our measurements show inconsistencies though, which we attribute to manufacturing imprecisions.

[4]We use the Relative Standard Deviation for our evaluations, as it is more aligned with the relevant notion of signal-to-noise ratio.

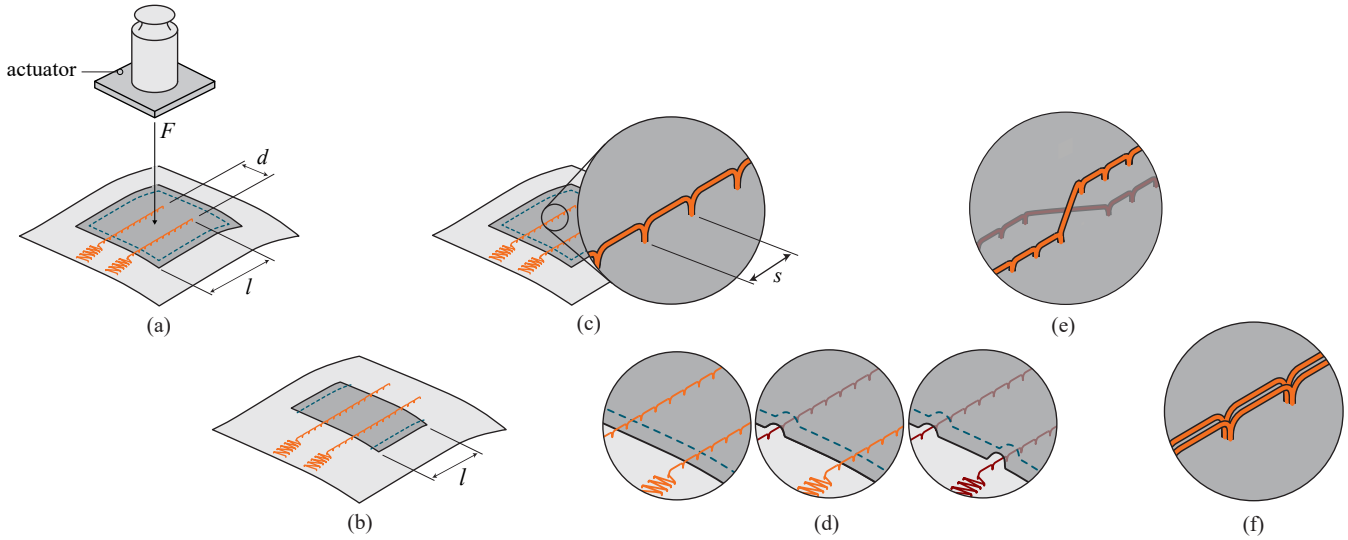

Figure 4: Variables of the sensor evaluation apparatus: electrode distance (a), electrode length (b), stitch length (c), electrode layering (d), electrode intersections (e), and double stitches (f).

We derive that electrode length can be used to counterbalance electrode distance, when designing a sensor patch. E.g. when higher electrode distance is required to fill larger sensor areas, increasing the electrode length is a means of cancelling out the rise of resistance, provided the nature of the pattern allows to do so.

4.3.3 Stitch length. Results of the stitch length experiment showed that patches with longer jumps showed higher resistance values at rest, which dropped significantly faster with pressure, when compared to shorter stitch lengths.

We argue that larger stitch lengths are preferable, as smaller jumps cause strong contact of yarn and resistive sheet already in resting state, which results in reduced dynamic range. However, choosing the stitch lengths too large may result in slack yarn, depending on the material, so it must be chosen with care. In contrast to electrode distance and length experiments, we observed relatively minor changes in the sensor's resting resistance when stitch length is modified (+8 % for 2 mm and +26 % for 5 mm, when compared against 1 mm patches).

4.3.4 Electrode Layering. We found that electrode layering substantially influences the sensing performance.

Patches with both electrodes *on top* showed the least dynamic range, since they were already in good contact with the resistive material at resting state. Samples with *mixed* order exhibited significantly higher drops in resistance as well as higher resting resistances. This trend extended to samples with both electrodes *below*, where both dynamic range and resting resistance were highest. Furthermore, we observed a remarkably high sensitivity, with relative resistance drops of 61 % (below) and 47 % (mixed), already when applying the actuator plate (12 g), against only 0.45 % for the reference patches (on top).

Although the *below* approach shows highest dynamic range and lowest sensitivity, the patch is of rather slack quality, as it tends to wrinkle and lose contact easily, which reflects in highly inconsistent readings for resting resistance (RSD = 26 %). Consequently, we consider the *mixed* approach to be a superior compromise in practice, as it also shows excellent performance and does not suffer from the issue of wrinkling, since the resistive material is fixed already by stitching an electrode on top. Additionally, it enables sensor patterns featuring intersecting electrode traces.

4.3.5 Intersections. Samples with a single intersection in general showed lower resistance when compared to ones with no intersections, with resistance drops of 18 % (resting), up to 58 % (2000 g). This result was expected due to the electrodes' low distance at the intersection point. Also, the dynamic range is affected, rising by 15 % in our tests, when comparing absolute differences between 0 g and 2000 g.

Summarizing, we found that intersections have to be handled with care, as they pose significant influence on both resting resistance and dynamic range. We therefore recommend keeping the intersection count as low as possible.

4.3.6 Double Stitches. Double stitched electrodes also significantly affect both dynamic range and resting resistance. Resistance values drop by 28 % (2000 g), up to 32 % (resting). Dynamic range (again comparing absolute differences between 0 g and 2000 g) drops by 60 %, when contrasted to the single stitched patches. We hypothesize this reduction in resting resistance and dynamic range results from more compression of yarn and resistive sheet, which coincides with similar observations for a small stitch length, as elaborated above.

In light of these results, we recommend avoiding trace sections requiring double stitches as much as possible.

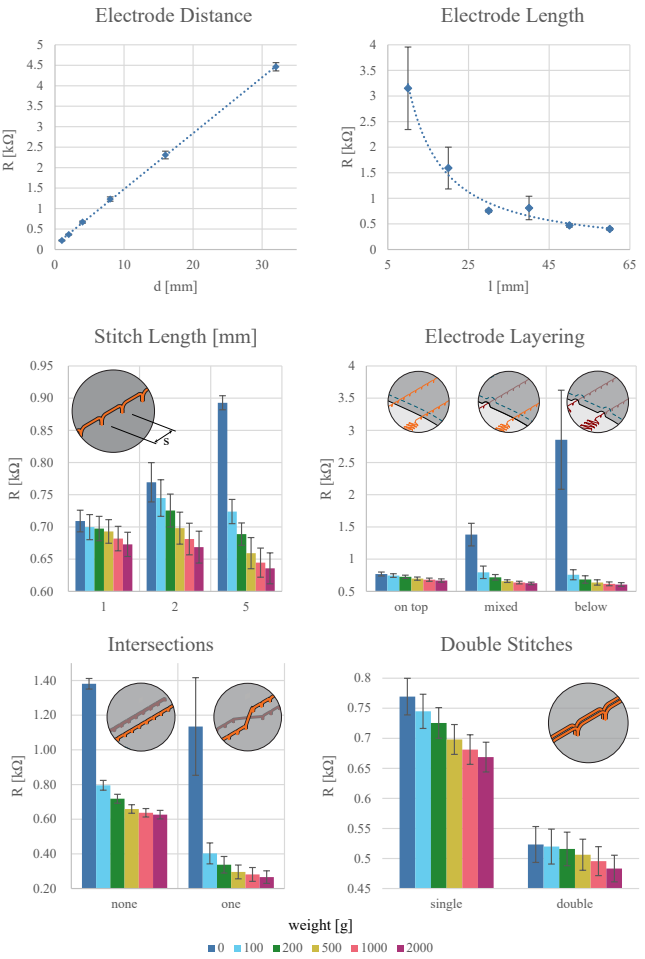

Figure 5: The results of our experiment with respect to the investigated parameters. Note that weight values on x-axes do *not* include the 12 g of the actuator plate.

5 SPACE-FILLING PATTERNS

As discussed earlier, we aim for finding sensor layouts, in order to cover multi-scale areas. Henceforth, we will call these layouts *patterns*, which are composed of two electrode *traces* (cf. Figure 6a). Depending on the geometric features, the resulting patterns may be used either as single sensor patches or as multiple linked (i.e. array or matrix) sensors (cf. Figure 6b). From related work, we identified the following, most essential requirements for our sensor layout:

Layout of alternating traces: To avoid areas with less sensitivity, the pattern should maximize the intervals where one electrode's trace is directly adjacent to the other electrode's trace, in contrast to running in parallel to itself.

Minimize segments requiring double stitches: Sections of double stitched traces (cf. Figure 6c) need to be minimized, as they not only require additional yarn but may also weaken the structural integrity of the resistive material, e.g. by perforating the sheet when stitch length is chosen too low. Also, we discovered an overall resistance drop, as can be seen in the previous chapter, effectively reducing the sensor's dynamic range.

Suitability for linkage of multiple sensors: Start and end of electrode traces are preferably located at the area's perimeter, so wiring of separate elements (e.g. electronics or adjacent patches) can be performed easily.

Uniform responsiveness: Ideally, the pattern provides a uniform, location-independent pressure response across the whole sensor area.

Feasibility for arbitrary size: Patterns allowing for arbitrary dimension are preferred, so patches can be easily adapted to fit in spatially constraining scenarios.

Minimum length of tracks: The lengths of electrode traces should be minimized, as additionally yarn increases costs and manufacturing time.

Support of arbitrary outlines and topologies: For maximum flexibility, the pattern should be adjustable for any outline shape, ideally even for concave shapes. In a best-case scenario, the pattern also supports arbitrary topologies, thus supporting shapes with holes and even nested sensitive areas.

5.1 Candidate Patterns

To infer an optimal layout, we investigated arrangements used in prior work [3, 37] in terms of the presented requirements. We closely examined several patterns (cf. Figure 7), including (i) *Interdigitated Electrodes*, (ii) *Boustrophedon Path*, (iii) *Meander*, (iv) *Fermat Spiral*, and (v) patterns derived from fractal space-filling curves, in particular from *Hilbert Curve*.

In order to generalize these patterns, we introduce the parameter *trace distance e* (cf. Figure 7), which is the minimum orthogonal distance between *electrode traces*. Note that due to the rather complex electrical implications of the patterns' geometries, both trace lengths and trace distance do *not* directly translate to the previously used parameters electrode length l and distance d from Equation 1.

5.1.1 Interdigitated Electrodes. We included the Interdigitated Electrodes (IDE), as it is widely used in commercial (printed) FSR sensors (cf. Figure 7a). It shows uniform responsiveness all over the area and can easily be adapted for many outline shapes. While optimal for printed sensors, in the context of embroidery there is the downside of large sections requiring double stitching, i.e. along the "prongs".

5.1.2 Boustrophedon Path. The Boustrophedon pattern features numerous electrode intersections, uniformly distributed across the sensor area, but does not require double stitches (cf. Figure 7b). Due to its traces running vertically and horizontally, a matrix layout can easily be implemented.

5.1.3 Meander. Inspired by the Greek fret design, the Meander pattern is widely used in capacitive sensors [18]. The pattern is comparatively yarn saving as it does not require double stitches whatsoever (cf. Figure 7c). A critical disadvantage is its highly non-uniform responsiveness due to the electrode intersection in the center, which prevents inferring objective pressure data. Like the Boustrophedon however, it can be easily used to create a matrix layout.

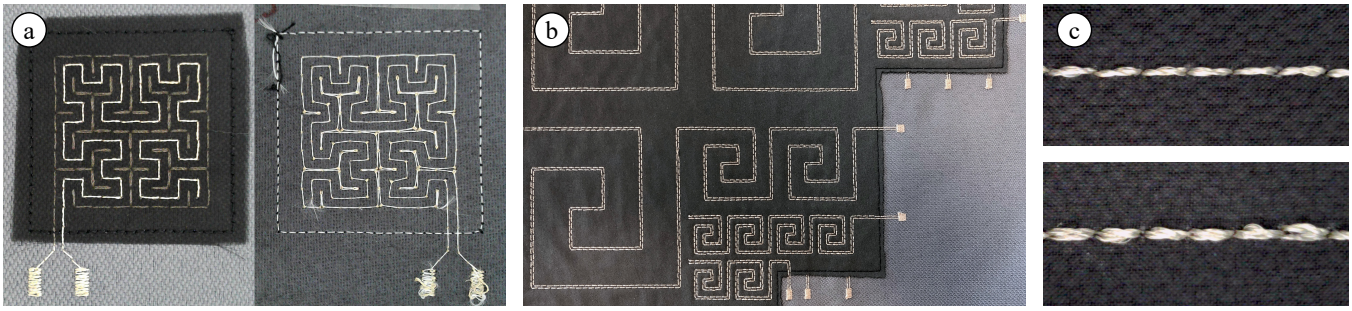

Figure 6: Top and bottom sides of the Hilbert Curve pattern (a). Depending on the pattern design, multiple tiles can be linked to arrays or matrices (b). Also, different scales can be combined, to gain areas with higher resolution. Single stitched electrode traces should be preferred over double stitched ones (c).

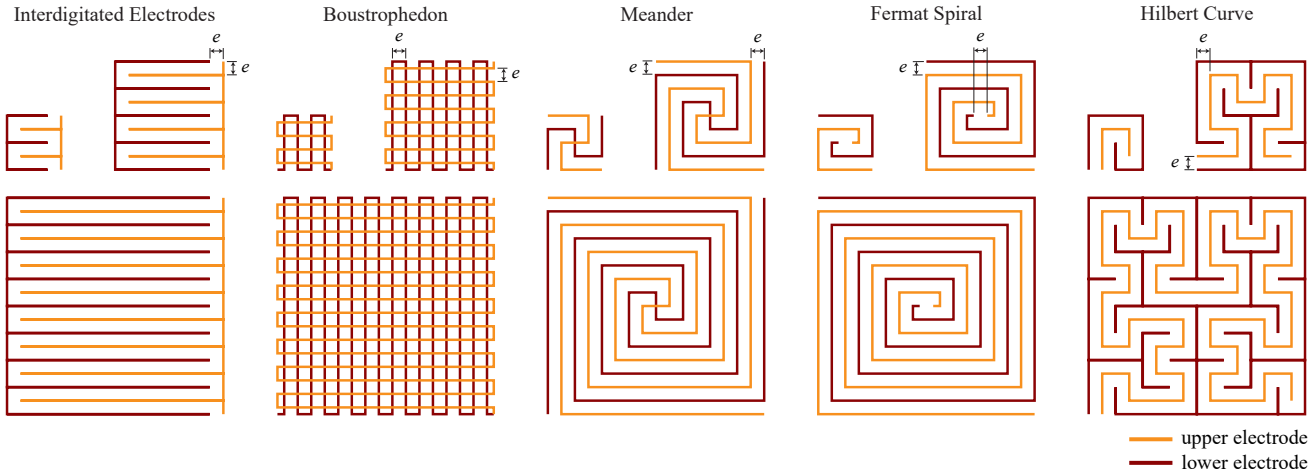

Figure 7: We investigated five different patterns, using 3 different sensor area sizes, while keeping trace distance e constant.

5.1.4 Fermat Spiral. A straightforward adaption of the Meander pattern, avoiding the unfavorable intersection, is the Fermat Spiral, with a division in the center to yield two separate electrode traces (cf. Figure 7d). In case of linking multiple patches, the trace ends should be located at the perimeter; therefore, the electrode must be stitched in both ways, thus requiring double stitching of the entire traces.

5.1.5 Fractal Space-Filling Curves. In geometry, numerous candidate space-filling curves exist, such as Peano, Hilbert, Moore, Sierpiński, Morton etc. Arguably, most of these patterns are very much interchangeable in our use case, since the respective electrodes' layout on the sensor area may be of little relevance, as long as trace lengths and trace distance are similar. Consequently, we selected based on a manufacturing point of view, e.g. *Gosper Curve* features a non-quadratic footprint and *Morton Curve* is hard to complement with a second electrode. We further evaluated both *Peano* and *Hilbert curves* and ultimately decided to choose the latter as its Euclidean length grows with curve order with 2^n, in contrast to the Peano's, which grows with 3^n. Therefore, the Hilbert curve is superior to the Peano curve in terms of scaling behavior, while similar in stitching trace and yarn usage.

6 PATTERN EVALUATION

We evaluated the five chosen patterns in a formal study. In total, we implemented 15 different samples (5 patterns × 3 sizes) and fabricated 3 samples for each to cancel out fabrication imprecisions in our data, resulting in an overall of 45 patches. We chose *mixed* electrode layering for all the pattern types, due to its good performance in the sensor evaluation, but also to be consistent with Meander and Boustrophedon, which inherently require this design, given the intersections. For all of the pattern types, we manufactured the most basic variants, thus disregarding additional double stitches of Fermat Spirals and Hilbert Curves, which would be required for linking multiple tiles.

Similar to the sensor evaluation, we fixed the CARBOTEX resistive fabric with a square of non-conductive yarn (42×42 mm^2). For evaluation, we mounted each of the samples flat on rubber sheet, and placed a PMMA-plate (5 g, 40×40 mm^2, so it would not rest on the fixation stitch) on top, for equally distributing pressure all

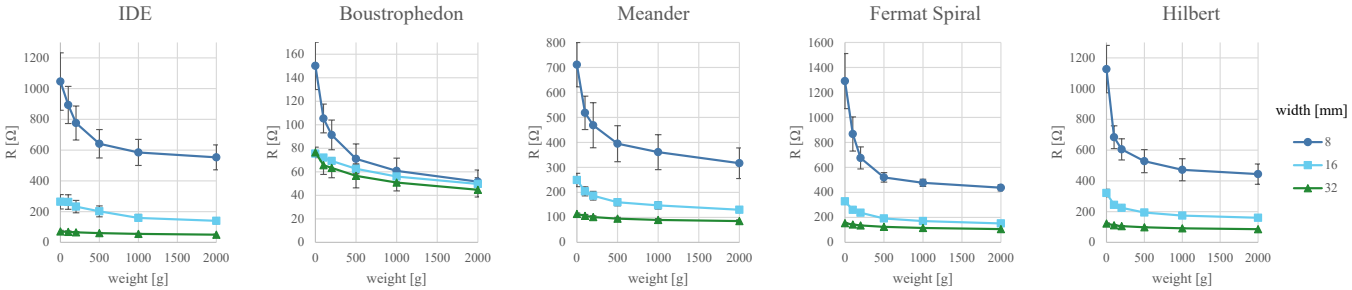

Figure 8: The results of our patches experiments show that Boustrophedon has particularly low resistance values. Especially trends for IDE, Fermat Spiral, and Hilbert Curve flatten out beyond 1000 g, making it particularly difficult to distinguish between high pressure values. Note that weight values on x-axes do *not* include the 5 g of the actuator plate.

over the sensor area. Again we placed weights of 100 g, 200 g, 500 g, 1000 g, and 2000 g.

Building on our earlier findings, we chose trace distance[5] e = 2 mm and stitch length[6] s = 4 mm, and varied sizes with w = 8 mm, 16 mm, and 32 mm, yielding three different curve orders (cf. Figure 7).

6.1 Results and Discussion

Overall, we did not remove outliers, as RSD was < 0.2% for all measurements. Figure 8 provides an overview of the results of the mean resistance values using different pressure levels. We observed that *Fermat Spiral* showed the highest dynamic range; the resistance dropped by 853 Ω, 177 Ω, and 47 Ω for the sizes 8 mm, 16 mm, and 32 mm respectively. Contrarily, relative dynamic ranges of all patterns are in similar ranges. As expected, *Boustrophedon* showed a very low resting resistance of 150 Ω, 76 Ω, and 77 Ω for pattern sizes of 8 mm, 16 mm, and 32 mm, due to numerous electrode intersections. This results in a particularly low signal-to-noise ratio and potentially challenges the measurement electronics. Similarly, the 32 mm variant of the *IDE* patch showed very low resistance values, starting at 81 Ω when no load applied.

We also noticed that the smallest samples (8 mm) showed highest deviation. We speculate that this is a result of manufacturing imprecisions, causing higher contributions to errors due to shorter traces, while similar flaws are canceled out in larger samples.

As expected, overall resistance dropped quickly with patch width, due to the quadratic growth of area and therefore trace lengths. In contrast to our previous experiment, we were not able to observe a proportional relation between resistance and electrode length. This seems reasonable given the high complexity of the current flow, resulting from intertwined electrode traces, high numbers of trace corners etc. We plan to further evaluate this in future work.

7 DESIGN RECOMMENDATIONS

Based on our two experiments that confirmed existing knowledge and brought new insights, we present the following design implications, for designers to consider when implementing pressure sensors using an embroidery machine.

[5]Note that with the exception of Boustrophedon, e is similar to electrode distance d as used in the sensor evaluation, however it does not directly translate.

[6]We state *maximum* stitch length, since not all stitches can have the same length; pattern layouts may occasionally dictate shorter stitches due to trace corners, dead ends, and intersections.

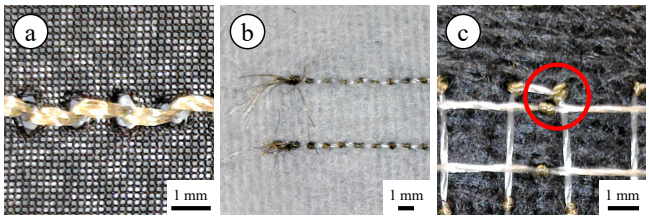

Figure 9: A too low stitch length may perforate the resistive sheet, seriously affecting its durability (a). When electrode yarn is trimmed, hardly visible fringes may cause shorts, so they must be carefully removed (b). Stitches must meet a reasonable distance and bobbin thread tension must be chosen accordingly, so the electrodes' loops at the patches' backsides do not short (c).

7.1 D1: Careful embroidery process

In general, embroidery is a very stressful process for both conductive and bobbin threads. Consequently, it causes yarn breakages, resulting in segmented circuit traces [12, 26]. Therefore, it is important to find a conductive thread which is explicitly designed to be used with an embroidery machine. As mentioned before, we found the Madeira HC40 as the most promising conductive yarn and during the implementation of all prototypes and samples, it has never broken. Additionally, we reduced the embroidery speed from a maximum of 800 stitches/min to 300 stitches/min, to avoid generated heat and friction. On the other hand, we noticed too low speeds causing the embroidery frame to oscillate, impairing the precision of stitches.

7.2 D2: Use a stabilizer

Stabilizer fabrics are used to enhance production quality and stability by reducing shimmy effects. Additionally, they provide adequate rigidity, which improves the sensor measurement quality. During our experiments, we tested numerous stabilizer fabrics that were placed at the bottom of the fabric. Even though it can be removed after the embroidery process, we keep it attached, since it prevents from warping the sensor, which would introduce noise in the resistance readings.

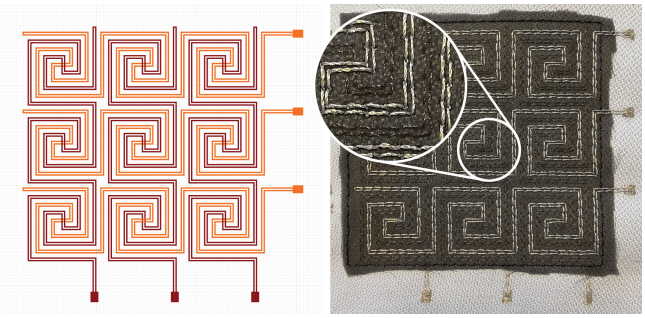

Figure 10: The Meander pattern can be used to build sensor matrices, as can any pattern with electrode intersections. Stitching a second, slightly offset backup trace for each electrode can improve durability.

7.3 D3: Optimize stitching settings

Depending on base and resistive materials, short stitches may be problematic as they would harm (e.g. perforate) the fabric (cf. Figure 9a). We established a borderline stitch length of 1 mm for the stitch we used in our test. Larger stitch lengths of 4 mm proved to be optimal for our sensor patches, as they resulted in sensors with reasonable dynamic range.

Thread tension balance should be considered to achieve a clean stitch backside. This is opposed to conventional embroidery for aesthetic means, where the backside is purely functional. Usually, the bobbin thread is supposed to hold the top yarn in place, e.g. by providing inwards tension in corners. In our case however, a clear trace is also required on the backside, as electrode yarn pulled out of place by the bobbin may cause shorts (cf. Figure 9c). Obviously, this issue is most prominent when using small electrode distances.

7.4 D4: Manufacture and finish carefully to avoid flaws

Trimmed yarn must be thoroughly verified and finished, as residual yarn is causing shorts. Some machines provide related system settings, however residue was still a few centimeters in length in our case. Even when we cut manually, hardly visible fringes easily cause shorts (cf. Figure 9b). This manual effort may be avoided by adapting the design to trim at an adequate distance or at safe areas, if possible.

For improved reliability, electrode traces may be stitched with two traces, running next to each other (cf. Figure 10). This way, a backup trace is added, so the sensor remains functional in case the electrode thread breaks. However, implications of this action must be considered, as it effectively reduces the trace distance and cuts the electrode resistances in half. Note that in contrast to double stitches, the two traces here run slightly offset, minimizing the damage inflicted on the resistive material.

7.5 D5: Choose an appropriate pattern

In our experiments, we showed that the sensing behavior of the patch can largely be controlled by choosing the pattern design, i.e. without adjusting components' materials or manufacturing procedures whatsoever. This gives some freedom of choice, since parameters can be adjusted so the resulting resistance range fits the requirements of the readout electronics. However, as we attribute the majority of pressure sensitivity to the interface effect, the electrode distance must be smaller than the minimum actuator size, since pressing between two traces will not reflect in measured resistance, and therefore dead spots will arise. The minimum trace distance is however dictated by the base and resistive materials' structure, e.g. yarn count—for our materials, we identified a 2 mm limit, unless mixed electrode layering is used, where even smaller distances may be feasible.

When trying new pattern designs, we recommend doing so with our earlier formulated layout requirements in mind.

7.6 D6: Linking of sensor patterns

The patterns presented in this paper pose different fitness for linking, which is a result of their electrode traces. Meander and Boustrophedon are suitable for building sensor matrices, as their traces run in orthogonal manner, thus vertically vs. horizontally, which is due to their intersection(s) (cf. Figure 10). Traces of IDE and Fermat Spiral on the other hand run in parallel, which is optimal for chaining, e.g. to build arrays. While fractal space-filling curves, such as Hilbert curves, are also chainable, they arguably are more appropriate for stand-alone patches.

7.7 D7: Fixing the hardware on the textile

To avoid fragile connectors, we recommend mounting the hardware to the fabric by embroidering (cf. Figure 11). The most critical part when fixing the hardware on the textile with the embroidery machine is the proper alignment and fixation of the board, so the needle does not punch beyond the hole, causing damage.

8 APPLICATIONS

In this section we show three different example applications enabled by embroidered pressure sensors. To demonstrate the feasibility and scalability of this approach, we challenged two developers and one designer to implement three prototypes within one day each. Beforehand, we developed a custom PCB with connector holes of 3 mm diameter, with the purpose of directly attaching it to the textile, similar to the LilyPad Arduino mainboard (cf. Figure 11a), to avoid fragile connections between electrodes and hardware. The PCB features 16 transmitter and 16 receiver connectors, power and ground, as well as an I^2C interface. The transmitter and receiver ports enable to scan a sensor matrix with a maximum of 16 columns and 16 rows via a shift register (74HC595D) and a multiplexer switch (ADG1438BRUZ), resulting in 256 individual sensors. The board is designed for usage in combination with an ESP32 MCU, which provides a readout rate of 100 Hz. Measurements are taken by the MCU's ADC via a voltage divider, calibrated with a digital potentiometer (MCPT41050), acting as a pull-down resistor.

The group received the evaluation results of this paper as a foundation. All three demonstrators were fabricated using tools commonly available in a fablab.

In a first application, the group implemented a slider interface, consisting of eight sequentially chained Fermat Spirals (cf. Figure 11b). Accordingly, the textile did not behave as a smooth slider, but

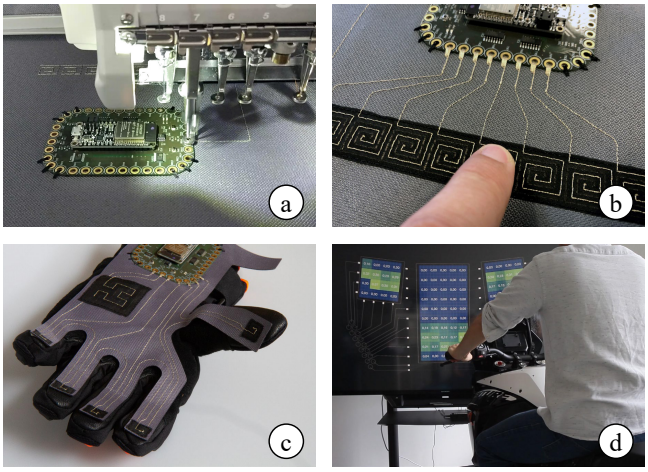

Figure 11: Our custom PCB was embroidered directly onto the fabric (a), to avoid fragile electrode connectors. Based on our findings, a simple slider (b), a motorcycle glove (c), and a seat cover (d) were created for demonstrating combinations of our sensors at different scales.

more like a set of individual buttons, which could be controlled individually; alternatively, a number of densely placed patterns (e.g. narrow IDE or Boustrophedon) could yield a higher spatial resolution.

In a second application, the same group designed and implemented a pressure-sensitive motorcycle glove (cf. Figure 11c). The team placed a 40×40 mm^2 2nd order Hilbert pattern on the palm and 16×16 mm^2 1st order Hilbert patterns on each of the glove's finger tips, as the positions of the pattern's electrode inlets are ideal for the wiring conditions at the fingertips. Also, the Hilbert pattern setup kept the amount of required conductive yarn low. All the sensor patterns were individually wired to the PCB, as the spatial separation does not require patch linking.

Finally, to demonstrate a large-scale setup, the group implemented a motorcycle seat cover (cf. Figure 11d), with the overall goal to analyze the biker's posture while riding. To provide an adequate spatial resolution, they linked sensors in a matrix layout for the seating area as well as for left and right thigh. While the reason for choosing *mixed* electrode layering in the first two was due to the higher resistivity, in this case it was inherently required, as electrode intersections are necessary to enable the matrix arrangements.

9 DISCUSSIONS AND LIMITATIONS

We discussed our sensor layout, design recommendations, and potential application scenarios. Expectedly, an embroidered pressure sensor does show limitations. Most of all, careful manufacturing is required. We also noticed hysteresis and drift; however, those effects were negligible, when compared to resistance readings. E.g. after a 10 s settling time, we observed a drift of just 0.6 % over a period of 1 h. More details can be found in the supplementary material.

The main limitation we identified is a rather inconsistent and non-deterministic performance, when compared to printed sensors. Reasons for this are found in irregularities of the manufacturing process, as well as material imperfections on a microscopic level, but also in physical composition innate to textile materials. E.g. after crimping or shearing, the sensor will hardly return to its exact previous state; hence slight shifts in characteristics are expected. Yet, the patches using space-filling patterns showed low standard deviation and therefore good part-to-part repeatability.

During our tests, we placed our patches on a rigid substrate, as otherwise applied force would be dodged, e.g. when applied on a pillow. Arguably, one of the key benefits of textiles – flexibility – is therefore limited, however numerous beneficial qualities remain, e.g. tactile quality. The resulting design possibilities are vast and beyond the scope of this paper.

Stretchability, which is a quality intrinsic to knits, is limited for our sensors due to the stabilizer required for the base material. Stretching would reflect in sensor readings indistinguishable from actual pressure. Consequently, the value of a stretchable pressure sensor using this approach is questionable.

We mentioned linking of multiple patterns to arrays or matrices, however this topic raises several challenges that are to be addressed in future work. Figure 6b shows an example of different scaled Meander patterns, linked on a single patch. Note that merging multiple smaller tiles into a big one does reduce yarn consumption but does not reduce readout complexity.

10 CONCLUSION & FUTURE WORK

We demonstrated the process of embroidering pressure sensitive sensors onto stabilized fabric, harnessing inherent advantages that derive from textiles, providing omnipresent, unobtrusive, breathable, flexible, and comfortable surfaces. We demonstrated that the practice of embroidering sensors provides huge benefits for rapid prototyping and bears great potential for customization.

For future work, we plan to investigate combinations of embroidered sensors with non-functional materials, not only for protective purposes, but to add valuable tactile qualities, e.g. by using deformable and elastic foams (e.g. ESD foam) as resistive material. Moreover, we plan to improve durability and possibilities for linking patches and connecting peripheral electronics. Finally, we strongly believe that adequate authoring tools are very essential for designers to come up with exciting ideas [4]. Therefore, we plan to implement a software solution for assisting in the processes of design, manufacturing, calibration, and operation.

We hope that our work, including complementary insights, will advance, encourage, and inspire the development of this exciting field, and that it will enable design and research communities to effectively implement textile pressure sensors by means of embroidery.

11 ACKNOWLEDGEMENTS

This research is part of the COMET project TextileUX (No. 865791, which is funded within the framework of COMET – Competence Centers for Excellent Technologies by BMVIT, BMDW, and the State of Upper Austria. The COMET program is handled by the FFG.

REFERENCES

[1] Bahaa Abbas, Salam K. Khamas, Alyani Ismail, and Aduwati Sali. 2019. Full Embroidery Designed Electro-Textile Wearable Tag Antenna for WBAN Application. *Sensors* 19, 11 (May 2019), 2470. https://doi.org/10.3390/s19112470

[2] Mohsen Akbari, Ali Tamayol, Veronique Laforte, Nasim Annabi, Alireza Hassani Najafabadi, Ali Khademhosseini, and David Juncker. 2014. Composite Living Fibers for Creating Tissue Constructs Using Textile Techniques. *Advanced Functional Materials* 24, 26 (July 2014), 4060–4067. https://doi.org/10.1002/adfm.201303655

[3] Humza Akhtar and Ramakrishna Kakarala. 2014. A comparative analysis of capacitive touch panel grid designs and interpolation methods. In *2014 IEEE International Conference on Image Processing (ICIP '14)*. IEEE, 5796–5800. https://doi.org/10.1109/ICIP.2014.7026172

[4] Lea Albaugh, Scott Hudson, and Lining Yao. 2019. Digital Fabrication of Soft Actuated Objects by Machine Knitting. In *Proceedings of the 2019 CHI Conference on Human Factors in Computing Systems (CHI '19)*. ACM Press, New York, NY, USA, 1–13. https://doi.org/10.1145/3290605.3300414

[5] Nicolas Brechet, Galatee Ginestet, Jeremie Torres, Elham Moradi, Leena Ukkonen, Toni Bjorninen, and Johanna Virkki. 2017. Cost- and time-effective sewing patterns for embroidered passive UHF RFID tags. In *2017 International Workshop on Antenna Technology: Small Antennas, Innovative Structures, and Applications (iWAT '17)*. IEEE, 30–33. https://doi.org/10.1109/IWAT.2017.7915289

[6] Jingyuan Cheng, Mathias Sundholm, Bo Zhou, Marco Hirsch, and Paul Lukowicz. 2016. Smart-surface: Large scale textile pressure sensors arrays for activity recognition. *Pervasive and Mobile Computing* 30 (Aug. 2016), 97–112. https://doi.org/10.1016/j.pmcj.2016.01.007

[7] Maurin Donneaud, Cedric Honnet, and Paul Strohmeier. 2017. Designing a Multi-Touch eTextile for Music Performances. *NIME 2017 Proceedings of the International Conference on New Interfaces for Musical Expression* (2017), 7–12. https://www.nime.org/proceedings/2017/nime2017_paper0002.pdf

[8] Franklin N. Eventoff. 1983. Electronic pressure sensitive force transducer. Patent No. US4489302A, Filed Sept. 24th., 1979, Issued March 15th., 1983.

[9] Mikhaila Friske, Shanel Wu, and Laura Devendorf. 2019. AdaCAD: Crafting Software For Smart Textiles Design. In *Proceedings of the 2019 CHI Conference on Human Factors in Computing Systems (CHI '19)*. ACM, New York, NY, USA, Article 345, 13 pages. https://doi.org/10.1145/3290605.3300575

[10] Ramyah Gowrishankar and Jussi Mikkonen. 2013. Pattern resistors. In *Proceedings of the 17th annual international symposium on International symposium on wearable computers (ISWC '13)*. ACM Press, New York, NY, USA, 137. https://doi.org/10.1145/2493988.2494341

[11] Nur Al-huda Hamdan, Jeffrey R Blum, Florian Heller, Ravi Kanth Kosuru, and Jan Borchers. 2016. Grabbing at an angle: menu selection for fabric interfaces. In *ISWC*. ACM Press, 1–7. https://doi.org/10.1145/2971763.2971786

[12] Nur Al-huda Hamdan, Simon Voelker, and Jan Borchers. 2018. Sketch&Stitch. In *Proceedings of the 2018 CHI Conference on Human Factors in Computing Systems (CHI '18)*. ACM Press, New York, NY, USA, 1–13. https://doi.org/10.1145/3173574.3173656

[13] Branimir Ivsic, Davor Bonefacic, and Juraj Bartolic. 2013. Considerations on embroidered textile antennas for wearable applications. *IEEE Antennas and Wireless Propagation Letters* 12, January (2013), 1708–1711. https://doi.org/10.1109/LAWP.2013.2297698

[14] Thorsten Karrer, Moritz Wittenhagen, Leonhard Lichtschlag, Florian Heller, and Jan Borchers. 2011. Pinstripe. In *Proceedings of the 2011 annual conference on Human factors in computing systems (CHI '11)*. ACM Press, New York, NY, USA, 1313. https://doi.org/10.1145/1978942.1979137

[15] Joanne Leong, Patrick Parzer, Florian Perteneder, Teo Babic, Christian Rendl, Anita Vogl, Hubert Egger, Alex Olwal, and Michael Haller. 2016. proCover: Sensory Augmentation of Prosthetic Limbs Using Smart Textile Covers. In *Proceedings of the 29th Annual Symposium on User Interface Software and Technology (UIST '16)*. 335–346. https://doi.org/10.1145/2984511.2984572

[16] Lin Shu, Tao Hua, Yangyong Wang, Qiao Li, David Dagan Feng, and Xiaoming Tao. 2010. In-Shoe Plantar Pressure Measurement and Analysis System Based on Fabric Pressure Sensing Array. *IEEE Transactions on Information Technology in Biomedicine* 14, 3 (May 2010), 767–775. https://doi.org/10.1109/TITB.2009.2038904

[17] Torsten Linz, René Vieroth, Christian Dils, Mathias Koch, Tanja Braun, Karl Friedrich Becker, Christine Kallmayer, and Soon Min Hong. 2008. Embroidered Interconnections and Encapsulation for Electronics in Textiles for Wearable Electronics Applications. *Advances in Science and Technology* 60 (Sept. 2008), 85–94. https://doi.org/10.4028/www.scientific.net/AST.60.85

[18] Bob Lee Mackey. 2006. Sensor patterns for a capacitive sensing apparatus. Patent No. US7129935B2, Filed June 2nd., 2003, Issued Oct. 31st., 2006.

[19] Viktorija Mecnika, Melanie Hoerr, Ivars Krievins, Stefan Jockenhoevel, and Thomas Gries. 2015. Technical Embroidery for Smart Textiles: Review. *Materials Science. Textile and Clothing Technology* 9 (Nov. 2015), 56. https://doi.org/10.7250/mstct.2014.009

[20] Jan Meyer, Bert Arnrich, Johannes Schumm, and Gerhard Troster. 2010. Design and Modeling of a Textile Pressure Sensor for Sitting Posture Classification. *IEEE Sensors Journal* 10, 8 (Aug. 2010), 1391–1398. https://doi.org/10.1109/JSEN.2009.2037330

[21] Robert H. Morris, Glen McHale, Tilak Dias, and Michael I. Newton. 2013. Embroidered coils for magnetic resonance sensors. *Electronics* 2, 2 (2013), 168–177. https://doi.org/10.3390/electronics2020168

[22] Patrick Parzer, Florian Perteneder, Kathrin Probst, Christian Rendl, Joanne Leong, Sarah Schuetz, Anita Vogl, Reinhard Schwoediauer, Martin Kaltenbrunner, Siegfried Bauer, and Michael Haller. 2018. RESi: A Highly Flexible, Pressure-Sensitive, Imperceptible Textile Interface Based on Resistive Yarns. In *Proceedings of the 31st Annual ACM Symposium on User Interface Software and Technology (UIST '18)*. ACM, New York, NY, USA, 745–756. https://doi.org/10.1145/3242587.3242664

[23] Patrick Parzer, Kathrin Probst, Teo Babic, Christian Rendl, Anita Vogl, Alex Olwal, and Michael Haller. 2016. FlexTiles: A Flexible, Stretchable, Formable, Pressure-Sensitive, Tactile Input Sensor. In *Proceedings of the 2016 CHI Conference Extended Abstracts on Human Factors in Computing Systems (CHI '16)*. 3754–3757. https://doi.org/10.1145/2851581.2890253

[24] Patrick Parzer, Adwait Sharma, Anita Vogl, Alex Olwal, and Michael Haller. 2017. SmartSleeve: Real-Time Sensing of Surface and Deformation Gestures on Flexible, Interactive Textiles, Using a Hybrid Gesture Detection Pipeline. In *Proceedings of the 30th Annual ACM Symposium on User Interface Software and Technology (UIST '17)*. https://doi.org/10.1145/3126594.3126652

[25] Irene Posch and Ebru Kurbak. 2016. CRAFTED LOGIC Towards Hand-Crafting a Computer. In *Proceedings of the 2016 CHI Conference Extended Abstracts on Human Factors in Computing Systems (CHI EA '16)*. ACM, New York, NY, USA, 3881–3884. https://doi.org/10.1145/2851581.2891101

[26] Ernest Rehmi Post, Margaret Orth, Peter Russo, and Neil Gershenfeld. 2000. E-broidery: Design and fabrication of textile-based computing. *IBM Systems Journal* 39, 3.4 (2000), 840–860. https://doi.org/10.1147/sj.393.0840

[27] Mahsan Rofouei, Wenyao Xu, and Majid Sarrafzadeh. 2010. Computing with Uncertainty in a Smart Textile Surface for Object Recognition. In *Proceedings of the IEEE International Conference on Multisensor Fusion and Integration for Intelligent Systems*. 174–179. https://doi.org/10.1109/MFI.2010.5604473

[28] Jose Saenz-Cogollo, Massimiliano Pau, Beatrice Fraboni, and Annalisa Bonfiglio. 2016. Pressure Mapping Mat for Tele-Home Care Applications. *Sensors* 16, 3 (March 2016), 365. https://doi.org/10.3390/s16030365

[29] Stefan Schneegass and Alexandra Voit. 2016. GestureSleeve: using touch sensitive fabrics for gestural input on the forearm for controlling smartwatches. *Proceedings of the 2016 ACM International Symposium on Wearable Computers (ISWC '16)*, 108–115. https://doi.org/10.1145/2971763.2971797

[30] Ali Shafti, Roger B. Ribas Manero, Amanda M. Borg, Kaspar Althoefer, and Matthew J. Howard. 2017. Embroidered Electromyography: A Systematic Design Guide. *IEEE Transactions on Neural Systems and Rehabilitation Engineering* 25, 9 (2017), 1472–1480. https://doi.org/10.1109/TNSRE.2016.2633506

[31] Axel Spickenheuer, Martin Schulz, Konrad Gliesche, and Gert Heinrich. 2008. Using tailored fibre placement technology for stress adapted design of composite structures. *Plastics, Rubber and Composites* 37, 5 (June 2008), 227–232. https://doi.org/10.1179/174328908X309448

[32] Mathias Sundholm, Jingyuan Cheng, Bo Zhou, Akash Sethi, and Paul Lukowicz. 2014. Smart-mat: Recognizing and counting gym exercises with low-cost resistive pressure sensing matrix. *Proceedings of the 2014 ACM International Joint Conference on Pervasive and Ubiquitous Computing (UbiComp '14)* (2014), 373–382. https://doi.org/10.1145/2632048.2636088

[33] Aris Tsolis, William Whittow, Antonis Alexandridis, and J. Vardaxoglou. 2014. Embroidery and Related Manufacturing Techniques for Wearable Antennas: Challenges and Opportunities. *Electronics* 3, 2 (May 2014), 314–338. https://doi.org/10.3390/electronics3020314

[34] Mark Weiser. 1999. The Computer for the 21st Century. *SIGMOBILE Mob. Comput. Commun. Rev.* 3, 3 (July 1999), 3–11. https://doi.org/10.1145/329124.329126

[35] Karsten Weiss and Heinz Wörn. 2005. The working principle of resistive tactile sensor cells. In *IEEE International Conference Mechatronics and Automation*. IEEE, 471–476. https://doi.org/10.1109/ICMA.2005.1626593

[36] Wenyao Xu, Ming Chun Huang, Navid Amini, Lei He, and Majid Sarrafzadeh. 2013. ECushion: A textile pressure sensor array design and calibration for sitting posture analysis. *IEEE Sensors Journal* 13, 10 (2013), 3926–3934. https://doi.org/10.1109/JSEN.2013.2259589

[37] Haisen Zhao, Fanglin Gu, Qi-Xing Huang, Jorge Garcia, Yong Chen, Changhe Tu, Bedrich Benes, Hao Zhang, Daniel Cohen-Or, and Baoquan Chen. 2016. Connected Fermat Spirals for Layered Fabrication. *ACM Trans. Graph.* 35, 4, Article 100 (July 2016), 10 pages. https://doi.org/10.1145/2897824.2925958

[38] Bo Zhou, Mathias Sundholm, Jingyuan Cheng, Heber Cruz, and Paul Lukowicz. 2016. Never skip leg day: A novel wearable approach to monitoring gym leg exercises. In *2016 IEEE International Conference on Pervasive Computing and Communications*. IEEE, 1–9. https://doi.org/10.1109/PERCOM.2016.7456520